Acoustic and thermal properties of silica aerogels and xerogels

S. Caponi,[1] G. Carini,[2] G. D'Angelo,[2] A. Fontana,[1] O. Pilla,[1] F. Rossi,[1] F. Terki,[3] G. Tripodo,[2] and T. Woignier[3]
[1]*INFM and Dipartimento di Fisica, Università di Trento, 38050 Povo, Trento, Italy*
[2]*Dipartimento di Fisica, Università di Messina, 98166 S. Agata, Messina, Italy*
[3]*Laboratoire des Verres, UMR 5587, Université Montpellier II, F34095, Montpellier Cedex, France*
(Received 2 April 2004; published 15 December 2004)

Comparative measurements of Brillouin light scattering and ultrasounds in a wide class of silica aerogels and xerogels show the existence of distinct mechanisms governing the temperature behaviors of the acoustic attenuation in the different frequency ranges. In the MHz range the attenuation is mainly regulated by dynamical mechanisms due (i) to thermally activated local motions of structural defects typical of vitreous silica at low temperatures and (ii) to relaxations of "extrinsic" defects at high temperatures, i.e., the hydroxyl groups covering the inner surface of the pores in aerogels. In the MHz range, instead, the attenuation is dominated by a temperature independent, or "static," process due to the scattering of phonons by pores. By growing the density of gels up to values close to that of dense vitreous silica, the acoustic attenuation shows a strongly temperature dependent behavior. The sound velocity scales with the density of the system following a power law, which is in good agreement with the predictions of a model describing silica gels in terms of a disordered network of microrods or microplates. The same law also permits to account for the temperature dependence of the sound velocity which reflects very closely the behavior observed in dense vitreous SiO_2. Finally the analysis of the low temperature specific heat (1.5–20 K) reveals that, for densities larger than about 1000 kg m^{-3}, the vibrational dynamics of these porous systems tends to reproduce the one of vitreous SiO_2.

DOI: 10.1103/PhysRevB.70.214204 PACS number(s): 61.43.Fs, 78.35.+c, 62.80.+f, 65.40.Ba

I. INTRODUCTION

It is well known that disordered solids exhibit properties in the low frequency vibrational dynamics which are not observed in their crystalline counterparts.[1–3] Among them, the specific heat of amorphous materials is much larger than the Debye value C_D,[4] the thermal conductivity shows a plateau between 5 and 20 K,[4] and the density of vibrational states, $g(\omega)$, exhibits a broad excess band in the plot of $g(\omega)/\omega^2$ referred to as Boson peak (BP).[5–7] The nature of these excess modes has been the object of different speculations particularly in the case of vitreous silica (v-SiO_2), which is considered the prototype of strong glasses. All these anomalies are usually ascribed to the nanometric length-scale and deal with the not yet completely understood vibrational dynamics of amorphous materials and in particular with the nature and the attenuation mechanisms of vibrational modes.[8–11] The questions at issue are without doubt relevant for the physics of disordered systems and a possible way to have an insight on this problem is the study of porous systems having a solid structure based on a connective backbone whose size can be reduced to a nanometric level. For this purpose, good candidate materials are silica aerogels and xerogels, highly porous solids whose density can be changed in the wide range from about 100 to 2200 kg/m^3. We have studied samples with densities in the range between 500 and 2200 kg/m^3, as a consequence of a controlled sintering procedure leading to modifications of their "texture" and of the network connectivity.[12,13] The sample density was always equal or greater than 500 kg/m^3 to avoid the fractal phenomenology. In light silica aerogels having a density lower than 500 kg/m^3, in fact, the dominant contribution to the vibrational dynamics has been attributed to localized modes (fractons), supported by a network having a fractal mass distribution over distances smaller than a characteristic length ξ (the size of the fractal cluster).[14] A well-defined phonon-fracton crossover, whose frequency increases with increasing density (or decreasing characteristic length), is exhibited in the density of vibrational states determined by inelastic neutron and Raman scattering.[15,16] In the frequency region below the phononfracton crossover corresponding to length scales larger than ξ, the aerogels can be considered as a system supporting the propagation of acoustic vibrations. Nevertheless, also samples with densities higher than 500 kg/m^3, show unexpected properties when compared to bulk glasses: (i) the low temperature specific heat is not always an excess respect to the Debye value C_D, but can be much lower than C_D;[17,18] (ii) the presence of strong quasielastic scattering in the low frequency region of the Raman and neutron spectra.[19–22] In addition to this, the inelastic characteristics (i.e., the dissipation mechanisms of elastic energy) of fractal and densified silica gels appear to be governed by the relaxations of locally mobile particles. Acoustic measurements carried out below 100 kHz in fractal silica aerogels in a restricted temperature range[23] were unable to establish if the observed relaxational contributions to the sound attenuation arise from the structural (bulk) defects of v-SiO_2, from surface relaxors or eventually from adsorbed molecules within the large surface of inner pores. Experiments of Brillouin spectroscopy performed in fractal and densified gels at room temperature[24,25] revealed the presence of relaxations tentatively ascribed to the organic groups covering the surface of the silica backbone. Now, ultrasounds and hypersounds by Brillouin light scattering probe the relaxation processes imposing their length scales in the experiment. The relevant length scale (i.e., the size of the relaxing molecular groups involved) is clearly of local nature, implying that the probe is

TABLE I. Density (ρ), index of refraction (n), average diameters of pores (L_p) and solid rods (L_s) diameters, the inner pores surface S and longitudinal sound velocity (V_l) in silica gels. The activation energies of the low (E_{act1}) and high (E_{act2}) temperature relaxations, the Debye velocity v_D and the Debye specific heat C_D/T^3 for some of the studied samples are also included.

Sample	Aerogel1	Aerogel2	Xerogel1	Xerogel2	Xerogel3	Densified Aerogel	v-SiO_2
$\rho(kg/m^3)\pm10\%$	690	800	510	770	1380	2190	2200
$n(\lambda=514.5$ nm)					1.29		1.46
L_p(nm)	14	-	12.3	6.6	3.5		
L_s(nm)	1	2.5	9	11	22		
$S(m^2/g)$	210	250	471	565	459		
v_l(m/s)	1870	2610	1254	2574	4064	5809	5983
v_D(m/s)	1241	1732			2715	4028	4132
$C_D/T^3(\mu J/gK^4)$[a]	91.1	28.9			4.35	0.84	0.77
$E_{act,1}/(kJ/mol)$		4.3					4.7
$E_{act,2}$(kJ/mol)		15			17		

[a]The transverse sound velocities of silica gels have been evaluated by considering $v_t/v_l=0.6$, this value representing an average of the ratios obtained in light aerogels (from Ref. 18) and in some sol-gel glasses (from Ref. 48).

sensitive to local motion within the system. The different mobility expected for the bulk and surface relaxors should lead to separate their relaxational contributions by an appropriate temperature and frequency investigation also permitting to characterize the underlying motions. Having this in mind, we investigated silica porous systems on different length scale using Brillouin light scattering and ultrasound measurements in a wide interval of temperature (5–800 K). Moreover, in order to monitor the influence of densification on the low energy vibrational dynamics and its relation with variations in the structural texture of the system, the low temperature specific heats of silica gels with increasing density have been determined. From the comparison between the results of Brillouin light scattering and ultrasonic measurements it has been found that the wavelength of the probe is a fundamental parameter to identify the different origins of the acoustic attenuation. Depending on the physical mechanisms regulating the acoustic energy dissipation, the attenuation can be strongly temperature dependent (*dynamic*) or temperature independent (*static*).

Using ultrasound ($\lambda\sim100$ μm), a dynamic attenuation behavior has been revealed even in the most porous sample, while a static of dynamic attenuation depending on the sizes of pores is observed using Brillouin light scattering ($\lambda=5145$ Å). The static or dynamical origin of the attenuation is ascribed to the interplay between the mean pore sizes of the samples and the probe wavelength. Moreover, upon samples with different degree of densification, the same probe detect a static to dynamical transition. The ultrasonic attenuation data reveal two distinct relaxation processes, one at low temperatures due to the thermally activated motions of bulk defects of vitreous SiO_2 and the other at temperatures close to room temperature due to surface relaxing groups. It has been also observed that the temperature dependence of the longitudinal sound velocity reflects very closely the behavior obtained in v-SiO_2, the differences in the magnitude of the velocity being regulated by the scaling properties of the elastic modulus with the density. To our knowledge the present study demonstrates for the first time that the density and temperature variation of elasticity of silica aerogels and xerogels are provided by the power law, which has been predicted by describing these systems in terms of a random network of solid rods.[17,26]

The paper is organized as follows: In Sec. II we describe the sample preparation and the experimental details. Section III contains the experimental results and the relative discussion, which is divided in three parts: the first regards the Brillouin light scattering experiment, the second ultrasonic measurements, and the third the low temperature specific heat. Basic conclusions are given in Sec. IV.

II. EXPERIMENTAL DETAILS

A. Samples preparation and characterization

Alcogels were prepared by hydrolysis and polycondensation reactions of tetramethoxysilane dissolved in methanol.[12] A set of xerogels with densities ranging between 500 and 1700 kg/m^3 was synthesized by aging the alcogels at 200 °C in autoclave at a pressure of 4 MPa. The obtained xerogels have surface areas covered by dangling bonds.[27] The porous structure absorbs H_2O molecules, which can be bonded to the surface (hydrogen-bonded silanols) or physically adsorbed.[27,29,28] To eliminate the most part of physical water,[19] the samples are heated at 600 °C for 24 h. The progressive densification of silica gels was obtained by thermal treatment in air for 72 h at several temperatures higher than 500 °C, reached with a heating rate of 0.1 °C/min. The heating process favors the removal of the free silanol groups (dangling Si-OH bonds) at pore surfaces causing cross-links between tetrahedra and reducing porosity. As reported in Table I, the density of the samples increased from $\rho=500$ kg/m^3 up to $\rho=2190$ kg/m^3. The latter sample, in the following named as densified aerogel, has been obtained by an annealing temperature of 875 °C.

The aerogels were prepared by a two step process: the supercritical drying necessary to synthesize aerogels is followed by a sintering in the temperature range 1000–1100 °C.[30] After the supercritical drying at 300 °C and 18 MPa for 3 h, aerogels have a macroscopic density ~300 kg/m^3. By a sintering heat treatment, the macroscopic density is almost 760 kg/m^3. Because of larger pore sizes, the aerogel samples have a smaller specific surface area and a smaller OH content.[31] The maximum of the pore size distribution is measured by nitrogen adsorption-desorption experiments[32] and the specific surface area, S, is obtained by BET analysis.[33] Some characteristics of aerogel and xerogel samples used in the present experiments are included in Table I.

B. Experimental set-up

Most of the Brillouin light scattering experiments are performed in backscattering configuration with a tandem six-pass Fabry-Pérot (FP) interferometer using different mirrors distances to have free spectral ranges (FSR) between 37.5 GHz and 7.5 GHz. The resolution, obtained by the width of the elastic peak, varies from ~500 MHz to ~100 MHz. A second high-resolution spectrometer consists of a double-pass plane FP interferometer, used as a prefilter, and a confocal FP, used as resolving unit (a more detailed description is given in Ref. 34). The free spectral range of the plane interferometer is equal to 75 GHz and finesse to 40; the frequency corresponding to the maximum transmission of the prefilter is matched with the frequency of the Brillouin line. The confocal FP, having a free spectral range of 1.48 GHz, is calibrated to scan only around the Brillouin peak; it has a finesse of 50, owing a total contrast of ~10^7.

The Brillouin shift, $\delta\omega_B$, is related to the sound velocity v and to the refractive index n of the studied material by the following expression:

$$\delta\omega_B = \frac{4\pi\nu_0}{c} v n \sin\frac{\vartheta}{2}, \tag{1}$$

where ν_0, c, and ϑ are the frequency of incident light, the light velocity and the scattering angle, respectively. By the Brillouin linewidth, Γ, the acoustic attenuation, α, and the inverse mean free path l^{-1} of hypersonic phonons can be determined by the following expression:

$$\alpha = l^{-1} = (4\pi\Gamma)/v. \tag{2}$$

The accuracy of the experimental data for the Brillouin shift and line width is, respectively, ±1% and ±5%.

The attenuation and the velocity of longitudinal waves was measured using a conventional pulse-echo ultrasonic technique the 15–30 MHz frequency range. The thermal scanning between 5 and 400 K was carried out by using a standard liquid helium cryostat in the range between 5 and 30 K and a cryogenerator between 15 and 400 K. The thermostatic control was better than 0.1 K in the whole temperature range.

The specific heat was measured in the range between 1.5 and 20 K using an automated calorimeter which operated by the thermal relaxation method, using a silicon chip as the sample holder on to which a sample of about 15–30 mg was bonded. The random error is apparent from the figures and any systematic errors are believed to be less than 3%–4%. To prevent undesirable effects of water moisture and adsorbed gas, all the Brillouin light scattering, ultrasonic and calorimetric measurements were performed by keeping the experimental chamber under a high degree of vacuum (about 10^{-6} mbar).

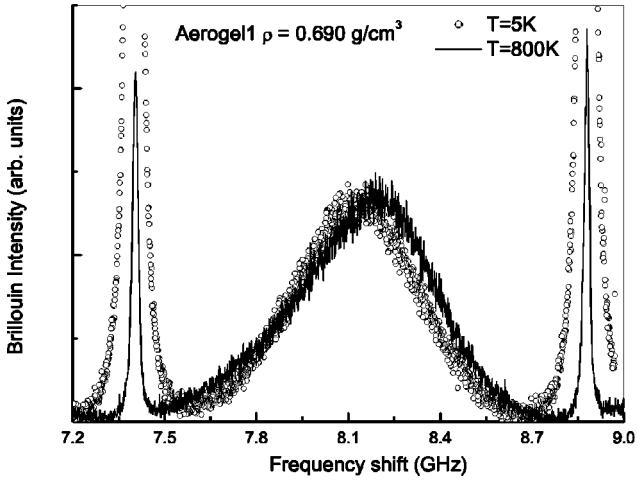

FIG. 1. Brillouin light scattering spectra at 5 K (open circles) and 800 K (solid line) in aerogel1. The comparison emphasizes the small shift of the Brillouin line and the inappreciable variation of the linewidth Γ with increasing temperature.

III. RESULTS AND DISCUSSION

A. Light scattering experiments

Figure 1 reports, as an example, experimental Brillouin light scattering spectra on silica aerogel1, collected at 5 K and 800 K with the spectrometer having the highest resolution. As already evident from the raw data, the spectral shapes are nearly identical showing that the acoustic attenuation is temperature independent. The weak shift shown in Fig. 1 is due to the temperature dependence of longitudinal sound velocity which reflects very closely that observed in v-SiO_2 as it will be shown in the following. The temperature dependence from 5 to 800 K of Brillouin linewidth Γ (half width at half maximum) for aerogel1, xerogel1, and the densified xerogel are compared to those of v-SiO_2 (Refs. 35–37) in Fig. 2. The behaviors observed in both densified sol-gel and v-SiO_2 show strongly temperature dependent attenuation. In v-SiO_2 it has been established that the sound attenuation is regulated by different dynamical mechanisms due to two-level systems ($T<10$ K) and to thermally activated relaxations of structural defects ($T>10$ K).[2,38] At variance aerogel1 and xerogel1 samples exhibit a temperature independent $\Gamma(T)$ even at lowest temperatures and an attenuation much higher than that of vitreous silica. The attenuation, α, is $\alpha = 7.3\cdot 10^4$ (db cm^{-1}) in aerogel1 and $\alpha = 7.0\cdot 10^4$ (db/cm^{-1}) in xerogel1. These values are much larger (one order of magnitude) than those measured at room temperature in vitreous silica and in densified xerogel (about

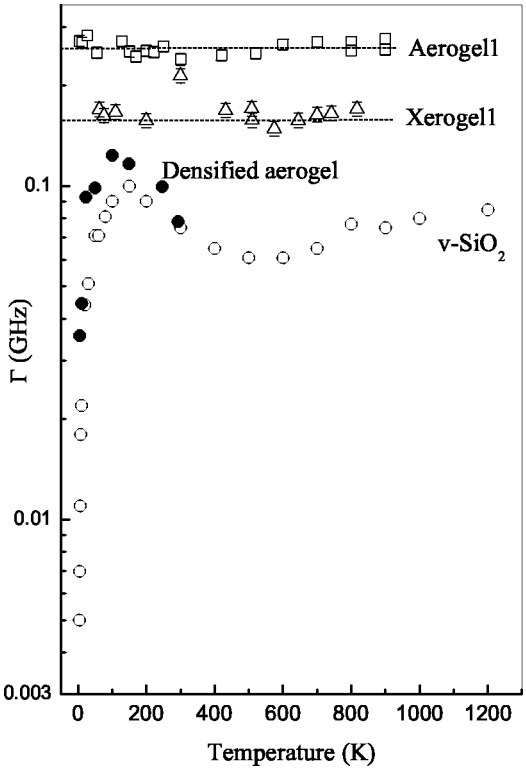

FIG. 2. Temperature behaviors of the half width half maximum of the Brillouin peak, Γ, in aerogel1 (□), xerogel1 (△), a densified aerogel (●), and v-SiO_2 (○) (from Ref. 36).

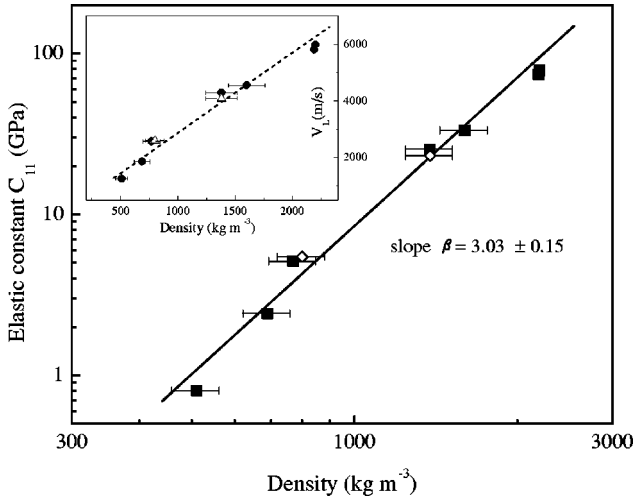

FIG. 3. The elastic constant C_{11} as a function of the density of aerogels and xerogels in a logarithmic plot. The solid line represents a fit to the experimental data giving the scaling exponent $\beta = 3.03 \pm 0.15$ (see text). In the inset the sound velocity is reported as a function of the density of aerogels, xerogels and v-SiO_2 in a linear plot. The open symbols are from ultrasonic measurements and the full symbols from Brillouin light scattering data. The characteristics of the samples are reported in Table I.

$7.0 \cdot 10^3$ db/cm^{-1} at a frequency of 34 GHz). The huge differences in the attenuation values can be explained considering that phonons in the porous media are continuously scattered by the discontinuities of the elastic constants between the bulk and pore parts. The above values demonstrate that the attenuation scales with the pore sizes (see Fig. 2 and Table I).[39] The effects of the wide distribution of pore sizes and of the multiple scattering of phonons contribute to the acoustic loss, leading to the observed values of attenuation. This evidences that the "classical" or Rayleigh scattering of thermal phonons by pores is the dominant mechanism of attenuation in the frequency range probed by Brillouin light scattering.[40] The longitudinal sound velocity, seems to follow a linear density dependence as shown in the inset in Fig. 3. This can be explained thinking that the porous materials are composed by a silica connective backbone surrounding by empty spaces. In fact, the problem of relating the microscopic structure of the porous material with its bulk properties, like sound velocity, was developed in the past and a density scaling law for the elastic modulus was proposed.[17,26] In the framework of a simple model of random networks of rods or plates, they obtained the density dependence of the elastic modulus M as given by the following expression:

$$M = M_0 \left(\frac{\rho^*}{\rho_0} \right)^{\beta}, \tag{3}$$

where ρ^* is the apparent (macroscopic) density of the silica gel, M_0 and ρ_0 the elastic modulus and the density of the material building massive part. Assuming that a similar relation is also valid also for the elastic constant $C_{11} = \rho v_1^2$, the following density dependence for the longitudinal sound velocity v_l is found:

$$v_l = v_{l,0} \left(\frac{\rho^*}{\rho_0} \right)^{\gamma}, \tag{4}$$

where $\gamma = (\beta - 1)/2$ and $v_{l,0}$ is the longitudinal sound velocity in vitreous silica. It is worth noting that from $\beta = 3.03 \pm 0.15$ obtained by the C_{11} behavior reported in Fig. 3, a value of 1.02 ± 0.08 is derived for γ. The power law which regulates the density dependence of the elastic modulus C_{11} has been previously observed to be valid in a very wide class of porous silica systems,[24] showing a small difference only in the scaling exponent ($\beta = 3.3$).

B. Ultrasonic experiments

Differently from the light scattering experiment, the temperature dependence of the attenuation measured in a ultrasonic frequency range show a dynamical behavior even on the most porous samples. The temperature dependencies from 5 to 400 K of the ultrasonic attenuation of silica aerogel2 at 15 and 25 MHz are shown in Fig. 4. As the temperature is increased from 5 K the attenuation increases up towards a broad peak, typical of oxide glasses,[2] whose maximum shifts to higher temperatures as the ultrasonic driving frequency is increased. Above about 200 K the attenuation starts to increase again showing a further large peak, also shifting to higher temperatures with increasing frequency. The velocity of 15 MHz longitudinal sound waves decreases from 5 to 40 K, exhibits a minimum at about 50 K and then rises about linearly with increasing temperature (inset of Fig. 4). Broadly similar results have been

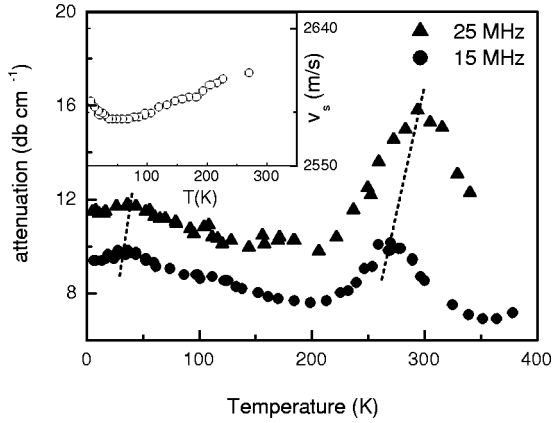

FIG. 4. Temperature dependence of the ultrasonic attenuation at 15 (●) and 25 (▲) MHz. In the inset, the longitudinal sound velocity at 15 MHz in aerogel2.

obtained for the attenuation and the sound velocity in silica xerogel3, even if the explored temperature range was more restricted (60–400 K). The temperature behaviors of the ultrasonic attenuation and longitudinal velocity for silica gels are compared to those observed in v-SiO_2 (Refs. 41 and 42) in Fig. 5. To make the comparison, the ultrasonic attenuation α has been transformed into the internal friction $Q^{-1}=2\alpha v/\omega$ and the velocity has been reported as the fractional sound velocity, i.e., $\Delta v/v_0=(v-v_0)/v_0$, being v_0 the value at the lowest temperature T_0 (5 K) in the experiment. The lowest value of α, i.e., that measured at the highest temperatures, has been subtracted to the experimental data as a background. It can be seen that the low temperature internal friction across the temperature range spanned by the broad peak is very similar in aerogel2 and in v-SiO_2, while the loss peak at higher temperatures, not observed in v-SiO_2, broadens with increasing density from aerogel2 to xerogel3 [inset in Fig. 5(a)]. The close similarity between the low temperature behaviors of the internal friction and the fractional sound velocity in aerogel2 and in v-SiO_2 is in accord with the hypothesis of a common origin for the revealed anomalies: below about 150 K, the acoustic behaviors are governed by thermally activated relaxations of the same intrinsic structural defects. The further loss peak observed above 200 K implies the introduction of supplementary degrees of freedom respect to the bulk material which can be attributed to extrinsic defects subjected to thermally activated local motions. In general, a relaxation rate of defects could be described by an Arrhenius law,

$$\tau^{-1}=\tau_0^{-1}\exp\left(\frac{-E_{\mathrm{act}}}{K_BT}\right) \tag{5}$$

and the plot of the frequencies versus the reciprocal temperatures of the acoustic loss maxima $(T_{\mathrm{peak}})^{-1}$, gives the average activation energies $E_{\mathrm{act},1}$ (low temperature peak) and $E_{\mathrm{act},2}$ (high temperature peak) reported in Table I. Also accounting for the roughness of the procedure (since the activation energy values are obtained by only two close frequencies), it is worth noting that the value of $E_{\mathrm{act},1}/k_B=4.3$ kJ/mol^2 is quite close to that obtained in vitreous silica over a very wide

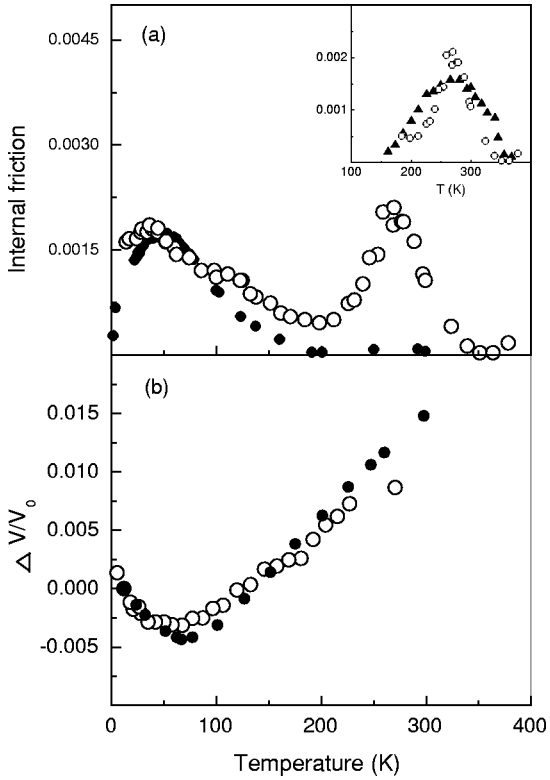

FIG. 5. (a) Comparison between the internal friction Q^{-1} for longitudinal 15 MHz ultrasounds in aerogel2 (○) and for longitudinal ultrasounds in v-SiO2 (●) (from Refs. 41 and 42). The inset shows the comparison between the high temperature relaxation peaks in aerogel2 (○) and xerogel3 (▲). (b) Comparison between the fractional sound velocity, $\Delta v/v_0=(v-v_0)/v_0$, for longitudinal 15 MHz ultrasounds in aerogel2 (○) and for longitudinal 6.8 MHz ultrasounds in v-SiO_2 (●) (from Ref. 42).

frequency interval ($E/k_B=4.7$ kJ/mol^2). The values of $E_{\mathrm{act},2}$ are in the range of energies usually characterizing the hydrogen bonding. It is believed that this latter relaxation process arises from local motions of the hydroxyl groups which cover the inner surface of silica gels. Among the different types of silanol species characterizing the silicate surface,[12] tentatively we associate this relaxation to the fraction of "*vicinal silanols*," i.e., OH^- groups which are bonded to surface silicon atoms having three bridging oxygens and can experience hydrogen bonding. It is to be noted, however, that the loss peaks cannot be explained in terms of a single relaxation time, as provided by the well known Debye equation, and therefore their accurate description should in general be obtained by considering a distribution of relaxation times arising from the inherent structural randomness of these systems. The larger width of the high temperature peak in xerogel3 as compared to that in aerogel2 [inset Fig. 5(a)] surely reflects a more complex distribution of local environments of the relaxors (the OH^- groups) probably arising from the smallest sizes of the pores and to the larger specific surface area of this sample. Since the low temperature attenuation shows a dynamic behavior which is quite similar in both v-SiO_2 and porous systems, this implies that, as also expected by the frequency dependence of Rayleigh scattering,

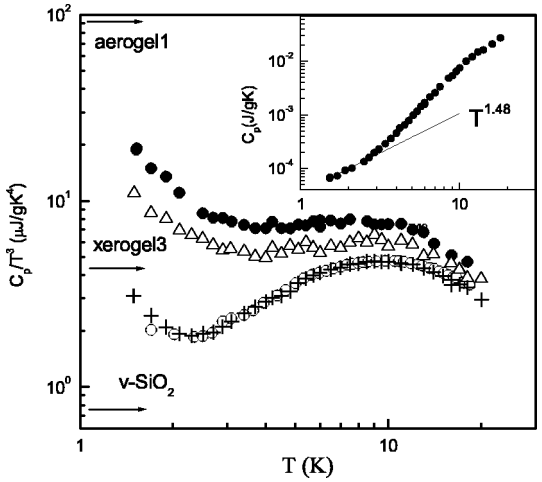

FIG. 6. Temperature dependence of C_p/T^3 for (○) v-SiO_2, (+) a densified xerogel, (△) xerogel3 and (●) aerogel1. The arrows show the Debye contributions C_D/T^3 calculated from sound velocity data (see Table I). The inset shows the temperature dependence of the specific heat C_p in aerogel1. The solid line represents a temperature variation having an exponent of 1.48.

this static contribution become negligible at ultrasonic frequencies.[40]

In close analogy to the internal friction, also the temperature dependencies of the fractional sound velocity in aerogel2 and v-SiO_2 [Fig. 5(b)] are nearly coincident, a significant deviation being observed only at temperatures above 250 K where the influence of the dispersion due to the high temperature relaxation process becomes dominant. The room temperature sound velocities measured in ultrasonic range, reported as triangles in Fig. 3, confirm the results obtained by Brillouin light scattering. It is worth noting that the relation (3) also permits is to obtain the temperature dependence of v_l. Since ρ^* is proportional to ρ_0 by a proportionality coefficient which is essentially given by the square of the ratio between the diameter d and the length l of a rod,[17] the quantity in parentheses in Eq. (3), can be considered as temperature independent coefficient and it represents only a scaling factor for the density variation of the sound velocity. Consequently $v_l(T)$ should reflect straightforwardly $v_{l,0}(T)$, as observed from the comparison of their experimental behaviors reported in Fig. 5(b).

C. Specific heat

In order to investigate the effects of the porous structure on the total density of vibrational states, the specific heat was measured on these systems. The experimental specific heats, obtained between 1.5 and 20 K for aerogel1 and xerogel3 and plotted as C_p/T^3, are compared to those of the densified xerogel and of v-SiO_2 (Spectrosil-B glass,[43]) in Fig. 6. Xerogel3, the densified xerogel and v-SiO_2 exhibit an excess specific heat over the Debye contributions C_D/T^3 (arrows in Fig. 6), having the characteristic shape (for a glass) of a broad peak. The Debye contributions have been evaluated by the classical relation

$$\left(\frac{C_D}{T^3}\right) = \frac{2\pi^2 k_B{}^4}{5\rho\hbar^3}\left[\frac{1}{3}\left(\frac{1}{v_L{}^3}+\frac{2}{v_T{}^3}\right)\right], \tag{6}$$

where the term in parenthesis in the r.h.s. is the inverse of the cubic power of the average Debye sound velocity v_D (see Table I) and the other parameters have their usual meaning. The effect of increasing density is to progressively reduce the low temperature upturn, so that the densified sample has a C_p nearly identical to that of v-SiO_2. The specific heat of aerogel1 exhibits an upturn below 4 K and a peak at higher temperatures which are significantly larger than those observed in the more dense xerogel3. Differently from the other samples, however, $C_p(T)$ of aerogel1 is much smaller than the Debye limit in the whole temperature interval explored. The broad hump in C_p/T^3 is associated to additional low-energy vibrational states, which originate the so-called *boson peak* (BP) observed in the low energy region of inelastic neutron and light scattering spectra of glasses.[44,45] Now, the overlapping excess specific heats can be considered as an evidence for the same excess in the vibrational density of states. This result is due to the peculiarity that the thermal treatment causes cross-links between the SiO_4 units by removing the dangling Si-OH bonds and produces a glass having the same structure of v-SiO_2 at least over a length scale of nanometers. This indeed is the region of lengths associated with the low-energy additional vibrations. The bump in C_p/T^3 of xerogel3 is close to that observed in v-SiO_2, in the temperature range of the excess associated to the BP (i.e., around 10 K). This finding is in agreement with the observations obtained by neutron scattering experiments in the same sample of v-SiO_2 and in xerogels having densities ranging in a wide interval, where a BP having a similar shape to that of v-SiO_2 was found.[22] Taking all the data together we conclude that, in these studied porous systems, the disorder introduced by pores does not affect too much the excess vibrational density of states in the region of the BP because the extension of the intermediate range order in their solid phase is comparable to that of v-SiO_2. Significant differences between the behaviors of $C_p(T)/T^3$ are observed below about 5 K and arise from the contribution of the "two level systems (TLS)." These excitations, which are associated to the tunnelling motions of groups of atoms (or single atoms),[46] contribute to the specific heat below 1 K with an approximately linear term in temperature. The differences between the upturns of the xerogel3 and v-SiO_2 could be associated with variations in the TLS density. These additional excitations could be ascribed to the large number of OH^- groups, located at the pore surface, which cause also the high temperature relaxation (see Fig. 4). The limited temperature range explored (down to 1.5 K) prevents any quantitative evaluation of the magnitude of this linear term. Different considerations are necessary to account for the low temperature specific heat of aerogel1, which is much smaller than the Debye contribution in the whole temperature range investigated. This C_p behavior is reminiscent of those reported in a series of silica aerogels having density $\rho < 870$ kg/m^3, where the measured C_p are always less than C_D in a wide range of temperature (0.05–20 K).[17,18] These features have been exhaustively discussed assuming the existence of different dy-

namic regimes (phonons, fracton and particle modes) corresponding to different length-scale regions of a fractal structure.[18,47] A similar description can be also used for explaining the $C_p(T)$ behavior in aerogel1. In fact $C_p(T)$ exhibits a slope between 1.5 and 3 K ($C_p \propto T^{1.48}$, see the inset of Fig. 6), which increases markedly with increasing temperature above 3 K as a clear indication of an additional vibrational contribution overlapping to those (phonons and fractons) governing the dynamics at lower temperatures. It is worth to emphasize that the obtained power law is quite close to that observed below 3 K in two light aerogels ($C_p \propto T^{1.4}$) where the exponent has been related to the fracton spectral dimension.[18] This observation enables an interpretation of the experimental C_p in terms of a large density of vibrational excitations (fractons and particle modes) over the usual Debye phonons, induced by the fractal texture of aerogel1. Therefore the present analysis of the low temperature C_p leads to conclude that, for silica gels having densities higher than about 1000 kg/m^3, the drying shrinkage[12] improves the binding between neighboring sites preventing the formation of a fractal network. The resulting locally dense structures are characterized by a vibrational dynamics which tends to reproduce that of v-SiO_2, i.e., an excess of low energy vibrations over the Debye-type phonons.

IV. CONCLUSIONS

The whole of observations indicates that relevant variations are found in the behavior of sound attenuation depending on the probe frequency and on the sample density. Using ultrasound, a dynamical attenuation behaviour has been measured even in the most porous system, while Brillouin light scattering measurements, depending on the size of pores, a dynamic to static transition in the attenuation has been found.

Moreover all the investigated samples have a series of properties that can be deduced from those of v-SiO_2 accounting for their particular density. The absolute values of sound velocities scale with the density following a power law and the temperature dependence of the fractional sound velocities nearly coincide with the behavior observed in v-SiO_2. Furthermore the temperature dependence of the longitudinal sound velocity strictly reflects the behaviors observed in tetrahedrically bonded glasses [such as SiO_2 and BeF_2 (Ref. 2)] showing a minimum followed by a linear increase with increasing temperature. All these peculiarities indicate that the density is the appropriate scaling factor for the elastic characteristics of silica gels. The same consistency between porous and bulk silica results from the analysis of the ultrasonic attenuation: in the low temperature region, the attenuation exhibits a very close dynamical behavior in v-SiO_2 and in porous silica materials. These observations are consistent with a model that represents the microscopic structure of these porous materials as formed by a disordered network of massive branches surrounded by empty spaces. The branches are characterized by a given diameter and a density close to that of v-SiO_2. Hence the quantities measured in porous systems are quite similar to those of v-SiO_2 because they are related to bulk system and are not very much affected by pores. The BP measured by neutron scattering experiments[20] as well as the peak in C/T^3 at 10 K are a clear indication that the porous systems with a density higher than 1000 kg/m^3 have a vibrational dynamics similar to that of the bulk system. The shape and the magnitude of the specific heat measured in these samples near the maximum is a clear indication that the dynamics of porous systems follows closely that of the bulk system.

[1] For a review see, Philos. Mag. B (1999); Special issue: Seventh International Workshop on Disordered Systems, Andalo, 1999, guest editors A. Fontana and G. Viliani.

[2] S. Hunkinger and W. Arnold, in *Physical Acoustic*, edited by W. P. Mason and R. N. Thurston (Academic, New York, 1976), Vol. XII, pp. 155–215.

[3] S. R. Elliott, *Physics of Amorphous Materials* (Longman Group Limited, London, 1983).

[4] For a review see, *Amorphous Solids: Low-Temperature Properties*, edited by W. A. Phillips (Springer, Berlin, 1981).

[5] U. Buchenau, H. M. Zhou, N. Nucker, K. S. Gilroy, and W. A. Phillips, Phys. Rev. Lett. **60**, 1318 (1988).

[6] A. Fontana, F. Rocca, M. P. Fontana, B. Rosi, and A. J. Dianoux, Phys. Rev. B **41**, 3778 (1990).

[7] A. P. Sokolov, A. Kisliuk, D. Quitmann, and E. Duval, Phys. Rev. B **48**, 7692 (1993); A. Brodin, A. Fontana, L. Borjesson, G. Carini, and L. M. Torell, Phys. Rev. Lett. **73**, 2067 (1994); G. Carini, G. D'Angelo, G. Tripodo, A. Fontana, A. Leonardi, G. A. Saunders, and A. Brodin, Phys. Rev. B **52**, 9342 (1995-I).

[8] F. Sette, M. Krisch, C. Masciovecchio, G. Ruocco, and G. Monaco, Science **280**, 1550 (1998).

[9] O. Pilla, A. Cunsolo, A. Fontana, C. Masciovecchio, G. Monaco, M. Montagna, G. Ruocco, T. Scopigno, and F. Sette, Phys. Rev. Lett. **85**, 2136 (2000).

[10] M. Foret, R. Vacher, E. Courtens, and G. Monaco, Phys. Rev. B **66**, 024204 (2002).

[11] M. Arai, Y. Inamura, T. Otonomo, N. Kitamura, S. M. Bennigton, and A. C. Hannon, Physica B **263–264**, 268 (1999).

[12] C. J. Brinker and G. W. Scherer, *Sol-Gel Science* (Academic, New York, 1990).

[13] D. Levy and L. Esquivias, Adv. Mater. (Weinheim, Ger.) **7**, 120 (1995).

[14] Y. Kantor, in *Scaling Phenomena in Disordered Systems*, edited by R. Pynn and A. Skejltord (Plenum, New York, 1985), p. 391.

[15] R. Vacher, E. Courtens, G. Coddens, A. Heidemann, Y. Tsujimi, J. Pelous, and M. Foret, Phys. Rev. Lett. **65**, 1008 (1990).

[16] E. Courtens, J. Pelous, J. Phalippou, R. Vacher, and T. Woignier, Phys. Rev. Lett. **58**, 128 (1987).

[17] A. M. de Goer, R. Calemczuk, B. Salce, J. Bon, E. Bonjour, and R. Maynard, Phys. Rev. B **40**, 8327 (1989).

[18] A. Bernasconi, T. Sleator, D. Posselt, J. K. Kjems, and H. R. Ott, Phys. Rev. B **45**, 10 363 (1992).

[19] A. Fontana, M. Montagna, F. Rossi, M. Ferrari, J. Pelous, F. Terki, and T. Woigner, J. Phys.: Condens. Matter **11**, A207 (1999).
[20] A. Fontana, M. Montagna, F. Rossi, L. Righetti, G. Cicognani, A. J. Dianoux, and F. Terki, J. Non-Cryst. Solids **280**, 217 (2001); A. Fontana, M. Montagna, F. Rossi, M. Ferrari, J. Pelous, F. Terki, and T. Woignier, J. Phys.: Condens. Matter **21**, A207 (1999).
[21] S. Caponi, M. Ferrari, A. Fontana, C. Masciovecchio, A. Mermet, M. Montagna, F. Rossi, G. Ruocco, and F. Sette, J. Non-Cryst. Solids **307-310**, 135 (2002).
[22] G. Cicognani, A. J. Dianoux, A. Fontana, F. Rossi, M. Montagna, T. Scopigno, J. Pelous, F. Terki, J. N. Pilliez, and T. Woignier, Philos. Mag. B **79**, 2091 (1999).
[23] A. M. Zimmermann, J. Gross, and J. Fricke, J. Non-Cryst. Solids **186**, 238 (1995).
[24] F. Terki, J. Pelous, P. Dieudonne, and T. Woignier, J. Non-Cryst. Solids **225**, 277 (1998).
[25] E. Anglaret, J. Pelous, and L. H. Hrubesh, J. Non-Cryst. Solids **186**, 137 (1995).
[26] G. Deutscher, R. Maynard, and O. Parodi, Europhys. Lett. **6**, 49 (1988).
[27] R. K. Iler, *Chemistry of Silica* (Wiley, New York, 1979).
[28] C. Duverger, M. Ferrari, C. Mazzoleni, M. Montagna, G. Pucker, and S. Turrel, J. Non-Cryst. Solids **245**, 129 (1999).
[29] L. T. Zhuravlev, *The Surface Chemistry of Silica*, Proceedings of 'SILICA 98' Mulhouse, 1998, p. 293.
[30] T. Woignier, J. Phalippou, and M. Prassas, J. Mater. Sci. **25**, 3117 (1990).
[31] L. T. Zhuravlev, Langmuir **3**, 316 (1987).
[32] E. P. Barret, L. G. Joyner, and P. P. Halenda, J. Am. Chem. Soc. **73**, 373 (1951).
[33] S. Brunauer, H. Emmet, and E. Teller, J. Am. Chem. Soc. **60**, 309 (1938).
[34] H. Sussner and R. Vacher, Appl. Opt. **22**, 3815 (1979); R. Vacher, H. Sussner, and M. V. Schickfus, Rev. Sci. Instrum. **51**, 3 (1980).
[35] A. Pine, Phys. Rev. **185**, 1187 (1969).
[36] R. Vacher and J. Pelous, Phys. Rev. B **14**, 823 (1976).
[37] R. Vacher, H. Sussner, and S. Hunklinger, Phys. Rev. B **21**, 5850 (1980).
[38] For a review see, S. Hunklinger and M. von Schickfus, *Amorphous Solids: Low-Temperature properties*, edited by W. A. Phillips (Springer-Verlag, Berlin, 1981), p. 81.
[39] S. Caponi, A. Fontana, M. Montagna, O. Pilla, F. Rossi, F. Terki, and T. Woignier, J. Non-Cryst. Solids **322**, 29 (2003); S. Caponi, P. Benassi, R. Eramo, A. Giugni, M. Nardone, A. Fontana, M. Sampoli, F. Terki, and T. Woignier, Philos. Mag. B **84**, 1423 (2004).
[40] R. Truell, C. Elbaum, and B. B. Chick, *Ultrasonic Methods in Solid State Physics* (Academic, New York, 1969). p. 161.
[41] R. E. Strakna and H. T. Savage, J. Appl. Phys. **35**, 1445 (1964).
[42] R. Vacher, J. Pelous, F. Plicque, and A. Zarembovitch, J. Non-Cryst. Solids **45**, 397 (1981).
[43] N. Ahmad and Matiullah, Solid State Commun. **76**, 433 (1990).
[44] A. Fontana, F. Rossi, G. Carini, G. D'Angelo, G. Tripodo, and A. Bartolotta, Phys. Rev. Lett. **78**, 1078 (1997).
[45] V. K. Malinovsky, V. N. Novikov, P. P. Parshin, A. P. Sokolov, and M. G. Zemlyanov, Europhys. Lett. **11**, 43 (1990).
[46] For a review see, *Amorphous Solids: Low-Temperature Properties*, edited by W. A. Phillips (Springer, Berlin, 1981).
[47] Y. Tsujimi, E. Courtens, J. Pelous, and R. Vacher, Phys. Rev. Lett. **60**, 2757 (1988).
[48] J. M. Grace and A. C. Anderson, Phys. Rev. B **33**, 7186 (1986).